

The Inositol Trisphosphate Receptor Regulates a 50-Second Behavioral Rhythm in *C. elegans*

Paola Dal Santo,* Mary A. Logan,[†]
Andrew D. Chisholm,[‡] and Erik M. Jorgensen*[§]

*Department of Biology

[†]Neurosciences Program
University of Utah

Salt Lake City, Utah 84112-0840

[‡]Department of Biology

Sinsheimer Laboratories

University of California

Santa Cruz, California 95064

Summary

The *C. elegans* defecation cycle is characterized by the contraction of three distinct sets of muscles every 50 s. Our data indicate that this cycle is regulated by periodic calcium release mediated by the inositol trisphosphate receptor (IP₃ receptor). Mutations in the IP₃ receptor slow down or eliminate the cycle, while overexpression speeds up the cycle. The IP₃ receptor controls these periodic muscle contractions nonautonomously from the intestine. In the intestinal cells, calcium levels oscillate with the same period as the defecation cycle and peak calcium levels immediately precede the first muscle contraction. Mutations in the IP₃ receptor slow or eliminate these calcium oscillations. Thus, the IP₃ receptor is an essential component of the timekeeper for this cycle and represents a novel mechanism for the control of behavioral rhythms.

Introduction

Rhythmic behaviors are widespread among species, and the time scale of these rhythms ranges from seconds to years. These behaviors depend on an endogenous timekeeping mechanism to set the frequency of the rhythm. For example, the well-characterized circadian clocks of insects, plants, and mammals are based on the oscillation of gene and protein products in synchrony with 24 hr cycles of light and darkness (for a review, see Dunlap, 1999). The mechanisms regulating biological rhythms with cycle frequencies shorter than a day (ultradian rhythms) are not as well understood. Pharmacological and electrophysiological studies indicate that there are two general mechanisms regulating these faster rhythms: cell-intrinsic oscillations in membrane potential or multicellular pattern generators (Marder and Calabrese, 1996). For example, the vertebrate heartbeat is an ultradian rhythm in which the rate of muscle contraction is set by oscillations of the membrane potential in pacemaker neurons. At the molecular level, the changes in the membrane potential of these cells are driven by interactions among voltage-sensitive K⁺, Na⁺, and Ca²⁺ channels (Giles et al., 1986). Alternatively, behaviors with

stereotyped movements such as breathing, walking, or swimming are controlled by networks of neurons functioning as central pattern generators. The best-characterized examples of these include the pyloric movements of crustaceans, the leech heartbeat, and swimming in mollusks, lamprey, and *Xenopus laevis* larvae (for a review, see Arshavsky et al., 1997; Calabrese, 1995; Marder and Calabrese, 1996). In these cases, rhythmic activity of the pacemaker neurons depends on the intrinsic electrical properties of these cells as well as on synaptic interactions among the neurons.

Biological clocks are distinguished from simple rhythms in that they possess certain attributes in addition to a fixed period. Specifically, the timing of a particular rhythm may be said to be controlled by a clock if it remains constant in the absence of environmental cues, if it is unaffected by changes in temperature, and if the phase of the period can be synchronized (entrained) by environmental stimuli (Edmunds, 1988; Dunlap, 1993). In the nematode *Caenorhabditis elegans*, the defecation cycle is regulated by an ultradian clock (Thomas, 1990; Liu and Thomas, 1994). This behavior is characterized by the periodic contraction of three distinct sets of muscle: the posterior body muscles, the anterior body muscles, and the enteric muscles (Figure 1). These contractions occur approximately every 50 s, and the clock continues to keep time in the absence of food even though the muscle contractions are suppressed. In addition, the cycle time remains constant over a range of temperatures, and the phase of the cycle can be reset to the starting point by lightly touching the animal. These properties indicate that an endogenous clock regulates the frequency of the defecation cycle.

The cells that control the defecation cycle are unknown. Laser ablation experiments identified two motor neurons, AVL and DVB, that are required for the execution of the anterior body contraction and the enteric muscle contraction (McIntire et al., 1993). These data suggested that a neuronal circuit might function as a central pattern generator similar to that of other ultradian behavioral rhythms (Iwasaki et al., 1995; Iwasaki and Thomas, 1997). For the following reasons, however, it is unlikely that a neuronal central pattern generator controls the defecation cycle. First, extensive laser ablations of neurons did not affect either the posterior body contraction or the cycle time (E. M. J. and H. R. Horvitz, unpublished data). Second, mutations that disrupt neurotransmission also have no effect on the posterior body contraction and do not eliminate the cycle (P. D. S. and E. M. J., unpublished data). Together, these observations suggest that nonneuronal cells keep time and activate the posterior body contraction at the start of each cycle.

To identify the genes required for maintaining normal rhythm, Iwasaki et al. (1995) screened for mutants with abnormal defecation cycle times. Thirteen *dec* (defecation cycle defective) genes were identified in the screen, and the mutant phenotypes fell into two classes, termed *dec*-short and *dec*-long. As the names imply, *dec*-short mutations confer a shortened cycle time (25–40 s), while

[§] To whom correspondence should be addressed (e-mail: jorgensen@bioscience.utah.edu).

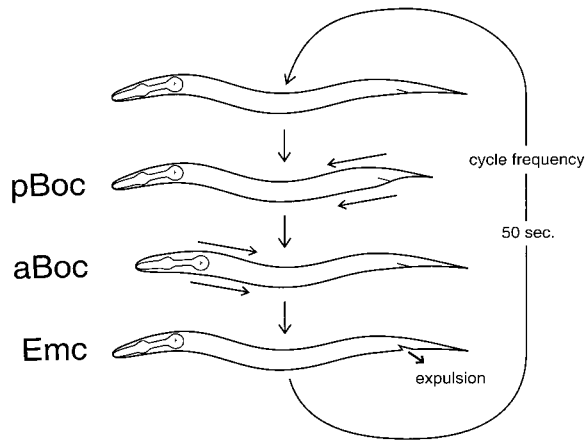


Figure 1. Schematic Diagram of the Defecation Cycle
Every 45–50 s a cycle is initiated by the posterior body wall muscle contraction (pBoc). Relaxation of these muscles is followed about 3 s later by an anterior body wall muscle contraction (aBoc) and, finally, 1/2 s later by the enteric muscle contraction (Emc) and expulsion of intestinal contents.

dec-long mutants have a long cycle time (60–90+ s). None of the mutations eliminate the cycle; therefore, it is not clear whether any of these genes encode essential components of the timekeeping mechanism or if they are simply modulators of cycle time. If there were a molecular timekeeper whose output determined cycle time, it could be defined in genetic terms as a locus that could be mutated to each of the following phenotypic states: no cycles, slow cycles, or fast cycles. Thus, the activity of this gene product would set the speed of the rhythm.

In this study, we identify a gene, *itr-1*, that is required for the timing of the defecation cycle. The *itr-1* gene encodes an inositol trisphosphate (IP₃) receptor, a protein involved in regulating intracellular calcium levels. In *C. elegans*, IP₃ receptor expression in the intestinal cells is necessary and sufficient to provide normal behavioral rhythms. In addition, we demonstrate that calcium oscillations occur in the intestine with peak calcium levels just prior to the first muscle contraction of the cycle. Thus, IP₃ receptor-mediated calcium release in a single cell type, the intestine, coordinates the multicellular responses of a complex behavior.

Results

dec-4(n2559) Mutants Fail to Initiate the Defecation Motor Program

The allele *n2559* was identified in a screen for lethal mutations (A. D. C. and H. R. Horvitz, unpublished data). Subsequent analysis demonstrated that these mutants develop at a slow rate, requiring about 5 days to develop to adulthood instead of the 3 days observed in the wild type. Furthermore, the mutants are sterile, have no observable defecation cycle, and, as a result, are severely constipated.

Further analyses demonstrated that *n2559* is a strong allele of the previously identified *dec-4* gene. First, we mapped the *n2559* allele to a small interval between *lin-45* and *unc-24* on chromosome IV (Figure 2A). Within

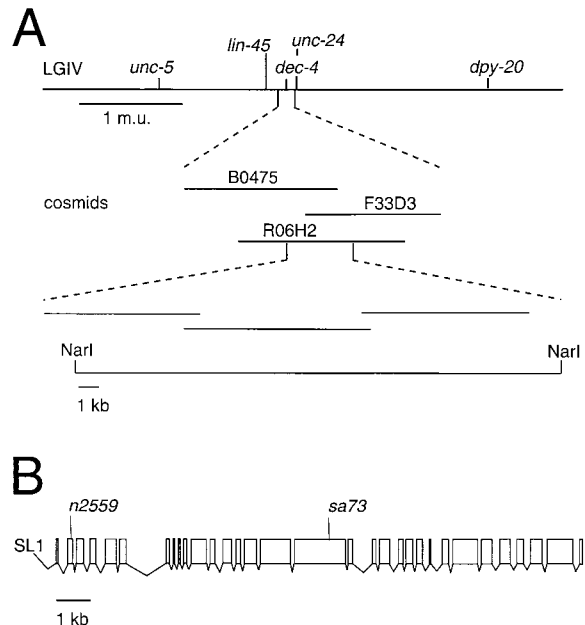


Figure 2. Genetic and Molecular Characterization of *dec-4/itr-1*

(A) Genetic and physical maps of the *dec-4* region. The mutations *sa73* and *n2559* genetically map to the interval between *lin-45* and *unc-24* on linkage group IV. The defecation cycle, fertility defects, and slow development of *n2559* and *sa73* mutants are rescued by the cosmid R06H2. Three overlapping fragments containing the *dec-4/itr-1* open reading frame and 7.4 kb of upstream sequence also rescue the mutant phenotypes associated with *n2559*. The overlap between fragments ranges from 400–800 bp. A 24 kb *NarI* restriction fragment containing the *dec-4/itr-1* open reading frame rescues the defecation cycle and sterility but not the slow development of *n2559* mutants.

(B) cDNA analysis of *dec-4/itr-1*. Exons are shown as closed boxes and introns as lines. The SL1 *trans*-spliced leader sequence is present on the 5' end of the *dec-4* message. The positions of mutations are shown.

this interval lies the *dec-4* gene, which is represented by a single allele, *sa73*. *dec-4(sa73)* was previously isolated in a screen for mutations with altered defecation cycle times (Iwasaki et al., 1995). The similarity in phenotype and map position suggested that *n2559* and *sa73* are alleles of the same gene. Consistent with this observation, *n2559* fails to complement *sa73*. Heterozygous animals (*n2559/sa73*) have an intermediate phenotype such that animals develop to adulthood, have a long defecation cycle time, and are sterile. By genetic criteria, *n2559* is a null allele: animals carrying the *sa73* mutation in *trans* to a deficiency have the same phenotype as *sa73/n2559* heterozygotes. Specifically, *sa73/stDf7* animals have a long defecation cycle time and are sterile. In addition, *n2559/stDf7* animals are indistinguishable from *n2559* homozygotes in that they lack defecation cycles and are sterile. These data demonstrate that *dec-4* is required for defecation cycle timing.

dec-4 Encodes an Inositol Trisphosphate Receptor

We cloned the *dec-4* gene using standard transformation rescue techniques. A single cosmid, R06H2, rescued the defecation cycle phenotype of *sa73* and *n2559* (Figure 2A). Rescuing activity of the *n2559* allele was

(inositol trisphosphate receptor/LET-23 fertility effector) by others (Fleming et al., 1996; Clandinin et al., 1998). To simplify the genetic nomenclature, we will refer to this locus as *itr-1*.

IP₃ receptors contain three functional domains: an amino-terminal ligand-binding domain, a central modulatory domain, and six carboxy-terminal membrane-spanning regions (Mikoshiba et al., 1994). The *C. elegans* protein is 38% identical to the mouse type 1 IP₃ receptor and 37% identical to the *Drosophila melanogaster* IP₃ receptor (Figure 3). This is the only IP₃ receptor sequence present in the *C. elegans* genome. The glycine residue that is altered in *n2559* is conserved in all species identified so far and affects the ligand-binding domain. The cysteine residue that is altered in *sa73* mutants is also conserved and affects the central modulatory domain of the protein. In other organisms, this domain is predicted to encode several important regulatory sites, including phosphorylation sites for cyclic AMP-dependent protein kinase A (PKA), protein kinase C (PKC), and Ca²⁺/calmodulin-dependent protein kinase II (CaMKII), as well as ATP, calmodulin, and Ca²⁺ binding sites (Ferris et al., 1991a, 1991b; Mikoshiba et al., 1994; Sienaert et al., 1997). The *sa73* mutation does not specifically affect any of these putative sites in the *C. elegans* protein, although it is possible that the mutation disrupts a secondary structure important for receptor modulation.

The IP₃ Receptor Regulates Defecation Cycle Time

The genetic definition of a timekeeper of the defecation cycle is a gene that can be mutated to confer aperiodic, slow, or fast defecation cycle phenotypes. The existing mutations in the IP₃ receptor partially satisfy these criteria (Figure 4A). First, the strong allele, *n2559*, eliminates the cycle. We scored eight *n2559* adults for 10–20 min each and failed to observe any defecation cycles. Expulsions were occasionally observed during routine manipulations of this strain; however, these were rare and were likely to be caused by simple pressure in the intestine, since no muscle contractions were associated with the expulsion (Thomas, 1990). Other behaviors are normal in this strain. The animals actively forage, the pharynx pumps in the presence of food, and locomotion is comparable to wild-type animals of the same age. These observations suggest that muscle contraction is normal but that timing is specifically impaired, since a defecation cycle is never initiated. Second, the weak *sa73* allele confers a slow but regular cycle period. *sa73* homozygotes have an average cycle time of 96.0 ± 4.0 s but are wild type with respect to locomotion, pharyngeal pumping, and foraging behavior. Finally, overexpression of the *itr-1* gene confers a fast cycle phenotype. Transgenic animals carrying a multicopy array of the *itr-1* gene have a fast cycle (37.6 ± 0.4 s) compared to the wild type (49.5 ± 0.4 s). Together, these results suggest that the IP₃ receptor is not simply a permissive element but, rather, that its output determines the speed of the clock. Thus, the IP₃ receptor is part of the time-keeping mechanism that regulates the defecation cycle.

In addition to the defecation cycle phenotype, mutations in the IP₃ receptor affect development and fertility. From the time of hatching, wild-type animals develop

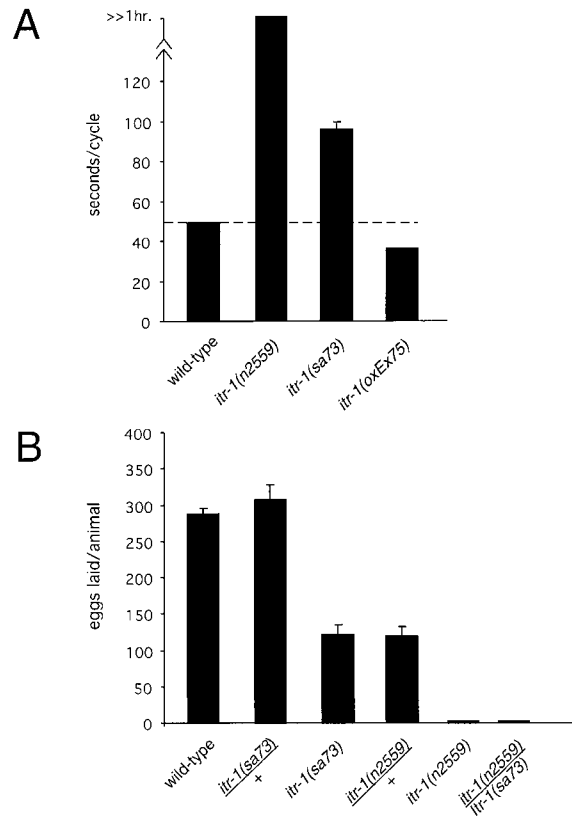


Figure 4. Phenotypic Characterization of IP₃ Receptor Mutants
(A) Defecation cycle times are altered in *itr-1* mutants. *itr-1(n2559)* strong mutants failed to initiate a cycle within 60 min of observation. *itr-1(sa73)* mutants have a long cycle time but maintain periodicity. Overexpression of *itr-1(+)* results in animals with fast cycle times. The mean and standard error are shown. The standard error for wild type and *oxEx75* are too small to be visible on this scale.
(B) Average brood sizes are reduced in *itr-1* mutants.

to adulthood in 3 days and produce about 300 progeny on average. *itr-1(n2559)* mutants develop to adulthood in about 5 days and are sterile. *itr-1(sa73)* mutants develop to adulthood in 3.5–4 days and have a reduced brood size (121 ± 9) compared to the wild type (287 ± 6 ; Figure 4B). Analysis of *n2559* mutants reveals that fertility may be sensitive to *itr-1* gene dosage. *n2559/+* heterozygotes have a reduced brood size (120 ± 8), as do *stDf7/+* deficiency heterozygotes (125 ± 43) (Clandinin et al., 1998; Figure 4B).

Mutations in the *C. elegans* IP₃ receptor were previously identified in a screen for effectors of an EGF receptor pathway involved in fertility (Clandinin et al., 1998). Five semidominant, gain-of-function alleles of the *itr-1* locus were selected based on their ability to suppress the sterility of an EGF (*lin-3*) mutant. We scored the defecation cycles of three *itr-1* gain-of-function alleles, and surprisingly, we did not observe any defects associated with timing of the cycle (*sy290*, 48 ± 0.6 s; *sy328*, 49 ± 0.3 s; *sy331*, 53 ± 0.3 s). This lack of phenotype might be explained by the molecular nature of the mutations. These mutations affect the amino-terminal ligand-binding domain of the IP₃ receptor; such changes

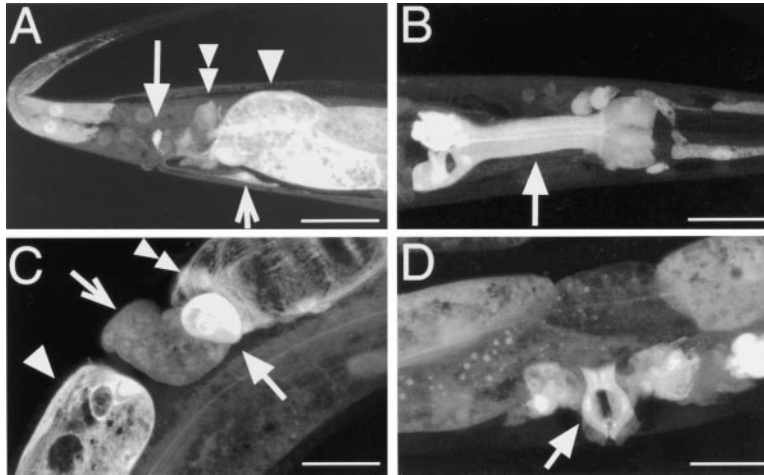


Figure 5. Expression Pattern of the *itr-1* Gene

Confocal images of transgenic animals expressing the *itr-1::GFP* fusion gene. The animals are oriented with the posterior at the left, anterior at the right, dorsal on the top, and ventral on the bottom.

(A) GFP is expressed in all intestinal cells (arrowhead), in the rectal epithelial (rep) cells (double arrowhead), the LUA neurons (closed arrow), and in the neuron PDA (open arrow). (B) GFP expression in the pharynx is restricted to the muscles of the metacarpus, isthmus, and the anterior portion of the terminal bulb (arrow).

(C) GFP is expressed in the gonad sheath cells (arrowhead), spermatheca (open arrow), spermathecal valve (closed arrow), and uterine sheath cells (double arrowhead).

(D) GFP is expressed in the vulval hypodermal cells (arrow). Bar, 30 μ m.

may not affect overall activity of the receptor in a wild-type background. However, our observations that *itr-1(n2559)* and *itr-1(sa73)* also affect fertility are consistent with the results implicating the IP₃ receptor in gonad function.

The IP₃ Receptor Is Expressed in Several Tissue Types

Our previous ablation studies were unable to identify the cells regulating cycle timing. To determine the cellular location of the rhythm, we constructed a transcriptional fusion containing 8.2 kb of 5' upstream sequence, and the first exon of *itr-1* fused to the coding region of green fluorescent protein (GFP). Transgenic animals that carry this construct show GFP expression in a variety of tissue types (Figure 5). Importantly in the context of this paper, GFP expression is observed in the intestine, and the posterior cells express GFP more intensely than the remaining intestinal cells (Figure 5A). Other cells include the rectal epithelial cells (Figure 5A), the pharynx (Figure 5B), the somatic gonad (Figure 5C), and vulval hypodermal cells (Figure 5D). In addition, the IP₃ receptor is expressed in hypodermal cells of the tail, rectum, and head. Pharyngeal expression is restricted to the muscles of the metacarpus, isthmus, and the anterior portion of the terminal bulb (m4, m5, and m6). Surprisingly, this construct was only expressed in two neurons (Figure 5A). In mammalian cells, IP₃ receptors display a more ubiquitous expression pattern, with highest levels in neurons, particularly in cerebellar Purkinje cells (Ferris and Snyder, 1992). It is possible that our fusion gene lacks a genomic regulatory element important for gene expression in neurons. However, neither *n2559* nor *sa73* mutants display locomotory defects. This lack of neuronal expression supports our previous observations that the cycle timing is not likely to be regulated by a neuronal network.

The IP₃ Receptor Functions in Intestinal Cells to Control the Defecation Cycle

The *itr-1::GFP* expression pattern narrowed the candidate cells, but it did not definitively establish the cellular focus of the oscillator. We used mosaic analysis

(Hedgecock and Herman, 1995) to determine the cells in which the IP₃ receptor functions to regulate the 50 s rhythm. We generated strains in which *itr-1(n2559) ncl-1* double mutants carried extrachromosomal arrays containing the *itr-1(+)* rescuing cosmid as well as the cell-intrinsic markers *sur-5::GFP* and *ncl-1(+)*. *sur-5::GFP* is a marker in which GFP is expressed brightly in the nuclei of most somatic cells, while *ncl-1(+)* rescues the abnormally large nucleoli of *ncl-1* mutants (Miller et al., 1996; Yochem et al., 1998). Therefore, the presence of the array in specific cells can be confirmed either by observing fluorescence in the nucleus or by observing the size of the nucleolus using differential interference contrast microscopy. We screened these strains for mosaic animals in which the extrachromosomal array had been lost in a subset of cells and scored the mosaic animals as either lacking defecation cycles (Dec) or having normal defecation behavior (non-Dec), as described in Experimental Procedures.

Analysis of the mosaic animals indicates that expression of the IP₃ receptor in the intestinal cells is necessary for cycle timing. We identified a total of 35 mosaic animals, including 27 Dec mosaic animals and 8 non-Dec mosaic animals (Figure 6). Loss of the array from the AB blastomere that gives rise to most neurons did not result in Dec animals (mosaic class m; see Figure 6 for details of mosaic classes). This lack of a role for neurons is consistent with our ablation studies and with the *itr-1::GFP* expression pattern. Loss of the array from the P₁ blastomere, on the other hand, resulted in Dec animals (classes a, e, and f). This lineage can be further subdivided, and we observed that losses in MS and P₂ that give rise to body wall muscles, some epidermal cells, the somatic gonad, and germline do not result in Dec animals (classes n and o). All animals with losses in EMS or its daughter cell E, which gives rise exclusively to gut, were Dec (classes b, c, h, d, and g). Furthermore, only animals with losses in these cells lacked cycles. Such a consistent pattern of array loss in the gut lineage suggests that IP₃ receptor function in the intestine is necessary for regulation of cycle timing.

Further analysis of non-Dec mosaic animals indicated that expression of the IP₃ receptor in the intestine is

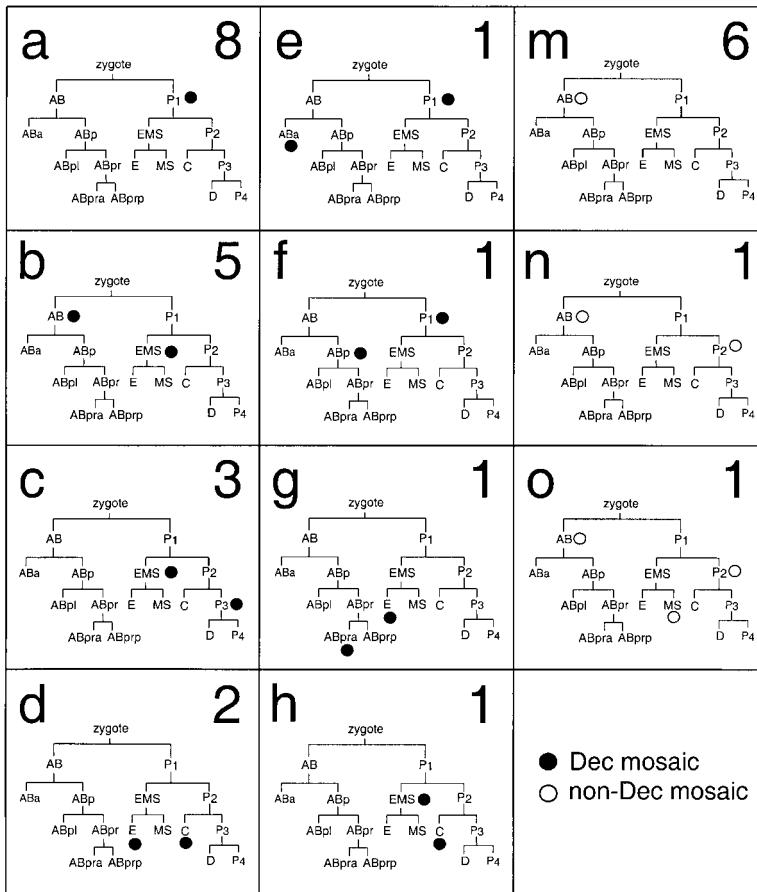


Figure 6. The Classes of *itr-1* Mosaic Animals Identified

Each class of mosaic is represented by a separate lineage. The point in the embryonic lineage at which the array was lost is indicated by closed circles for Dec mosaics and open circles for non-Dec mosaics. The number of animals in each class is indicated in the top right-hand corner of each box. Additional classes of Dec compound mosaics not shown in this figure are P₁ ABa ABpr (class i, n = 1), EMS ABprp (j, 1), E P₂ (k, 1) and E ABpl (l, 1).

sufficient for proper cycle timing. The two non-Dec mosaic animals in which the array was lost from AB and P₂ (class n) and AB, MS, and P₂ (class o) demonstrate that *itr-1(+)* expression in the intestinal cells is in fact sufficient for clock function. Most informative is the class of mosaic that retained the array only in the gut lineage yet had a normal defecation cycle (class o). Thus, these results indicate that the oscillator resides in the intestinal cells.

Calcium Spikes Occur at the Onset of a Posterior Body Contraction

The IP₃ receptor is known to function as an intracellular calcium release channel (Mikoshihba et al., 1994). Studies have shown that activation of the receptor results in the generation of intracellular calcium oscillations. Our finding that the IP₃ receptor functions in the intestinal cells to regulate the defecation cycle suggests a model in which calcium oscillations in the intestine trigger the defecation motor program. To test this hypothesis, we monitored calcium changes in the intestinal cells of living animals.

First, we observed calcium spikes in the intestine of wild-type animals. We injected the calcium-sensitive dye fura-2 into one of the two most posterior intestinal cells of adults. In eight animals that survived the injection, immobilization, and imaging procedures, calcium rises occurred in the injected cell. These rises in calcium were unlikely to be due to movement artifact, since the

increase in fluorescence due to calcium-bound fura-2 (fluorescence intensity measured at 340 nm) was accompanied by a decrease in fluorescence due to unbound fura-2 (fluorescence intensity measured at 380 nm). Moreover, there were no movements at the time of the calcium spikes in the corresponding images of the animals.

Second, the timing of calcium peaks was similar to the average defecation cycle time. In four out of eight animals, we observed a single peak in calcium followed by a single posterior body contraction during the time the animal was imaged (data not shown). In the remaining four animals, we observed multiple increases in fluorescence intensity, and the timing of each calcium peak was consistent with the timing of the defecation cycle (Figure 7A; see Experimental Procedures).

Third, calcium peaks occurred immediately before the onset of a posterior body contraction. In the experiment shown in Figure 7A, the tail of the animal was slightly mobile, allowing us to clearly observe the posterior body contractions that followed each calcium peak. In addition, posterior body contractions were observed using transmitted light following data collection, and the timing of the contractions remained in phase with the timing of the calcium peaks (pBocs e, f, and g). Figure 7B shows fluorescence micrographs of the tail in a series of four sequential images corresponding to the time points near peak b. In the first image, the tail is at rest. This is

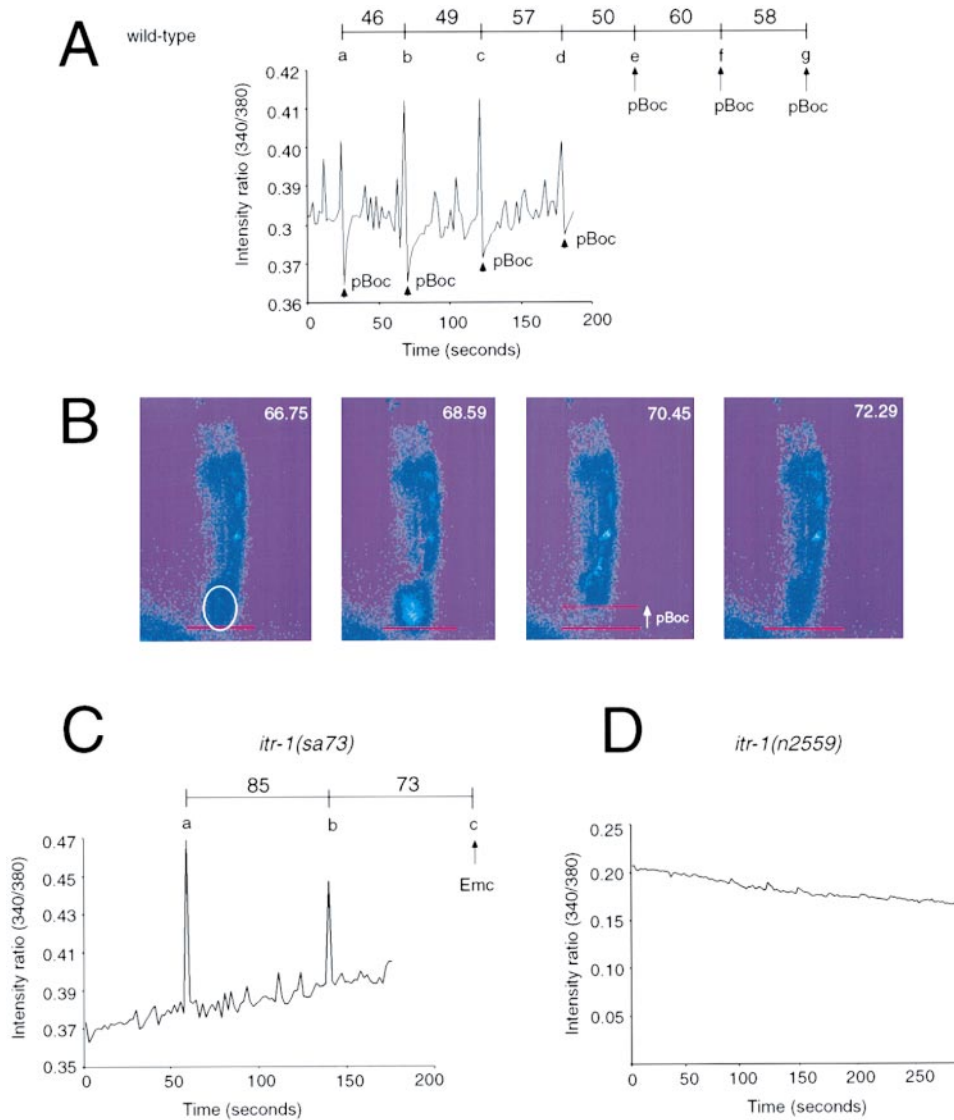


Figure 7. Calcium Oscillations in the Intestine Visualized with fura-2

(A) The wild type. Quantification of fluorescence intensities measured over a 3 min time period. The line above represents the time course of the experiment, beginning with the first peak of the first cycle. The start of each cycle is designated by a letter, and the duration in seconds of each cycle is shown. An arrow indicates that a posterior body contraction (pBoc) was observed during the experiment. Images were collected at approximately 2 s intervals. Posterior body contractions were observed postimaging, and cycle times are shown. The large peak just prior to the first pBoc is a movement artifact and can be distinguished from actual local increases in calcium by visual inspection of the images.

(B) Fluorescence micrographs corresponding to the animal imaged in (A). Specific time points are indicated in the top right-hand corner of each image. A red bar represents identical coordinates in each frame. A circle around the tail in the first image corresponds to the approximate area of integration used to measure fluorescence intensities.

(C) *itr-1(sa73)*. Images were collected as described for the wild type. An arrow indicates that an enteric muscle contraction (Emc) was observed after imaging.

(D) *itr-1(n2559)* mutants lack calcium spikes as well as posterior body contractions.

followed about 2 s later by an increase in calcium visible in the second image. In the third image, the posterior body muscles contract, and finally, in the fourth image, the tail returns to its original resting position.

As expected, the calcium oscillations were slowed or absent in the *itr-1* mutants. In the weak mutant, *sa73*, the average period between the calcium peaks was slow (80.3 ± 6.1 s) compared to the wild type (44.4 ± 2.5 s), and the peaks were in synchrony with the posterior body

contractions (Figure 7C). We did not detect any calcium oscillations in the strong allele *n2559* (Figure 7D). We observed six *n2559* animals for a period of 5 min each and recorded no calcium spikes. In each case, the animals were still alive and feeding at the end of the experiment.

Taken together, these data demonstrate that calcium oscillations in the intestine occur just prior to the initiation of each defecation cycle, consistent with our model for the role of IP₃ receptor function in the intestinal cells.

Discussion

In this study, we demonstrate that the *dec-4* gene is allelic to *itr-1*, the *C. elegans* inositol trisphosphate receptor. The phenotypes of mutants in this gene suggest that one role of the IP₃ receptor is to activate the defecation motor program at regular intervals. Mosaic analysis demonstrated that loss of the IP₃ receptor in the intestinal cells disrupts the behavioral oscillator. Moreover, calcium spikes can be observed in the intestine. These calcium spikes are correlated with the defecation cycle frequency and directly precede the initiation of the posterior body contraction.

The IP₃ Receptor and Generation of Cellular Calcium Oscillations

IP₃ receptors have been well characterized at the biochemical, cellular, and molecular levels (reviewed in Berridge, 1993, 1997). Activation of either tyrosine kinase receptors or G protein-coupled receptors leads to the activation of phospholipase C (PLC) and to the production of the second messengers IP₃ and diacylglycerol. Diacylglycerol activates PKC, while IP₃ binds to and activates the IP₃ receptor, a calcium release channel localized to the endoplasmic reticulum. Activation of the IP₃ receptor opens the channel and allows calcium to flow into the cytoplasm, which can then act on neighboring IP₃ receptors by a mechanism known as calcium-induced calcium release (CICR). Initial calcium release results in positive feedback on the channel activity. At higher concentrations, calcium becomes inhibitory and channels close (Bezprozvanny et al., 1991). This dependence on calcium concentration is thought to contribute in large part to the generation of temporally and spatially regulated calcium oscillations.

How does the IP₃ Receptor Keep Time?

Our analysis of *itr-1* mutants suggests that IP₃ receptor activity and calcium release is a determinant of defecation cycle frequency. There are two models that can explain how the IP₃ receptor might function as a 50 s clock. One model depends on the rate of receptor activation, while the second model depends on the rate of recovery following inactivation of the receptor.

In the first model, cycle timing depends on the time required to generate a threshold level of cytoplasmic calcium sufficient for triggering a calcium spike. Indeed, a rate-limiting step in the generation of calcium waves is the rate of calcium diffusion from one channel to neighboring channels (Wang and Thompson, 1995). When the IP₃ receptor was overexpressed, the frequency of the defecation cycle became faster. The increased number of IP₃ receptors caused by overexpression may cause a critical calcium level to be reached sooner and thereby increase the frequency of calcium spikes. Mutations in the IP₃ receptor that increase the cycle time may slow down the rate of calcium release either by affecting calcium conductance through the channel or by preventing a modification that may enhance channel activity. The *itr-1(sa73)* mutation lies in the central modulatory region of the protein and is not likely to affect conductance of the channel. Because the mutation is adjacent to a calcium-binding site identified

in the mouse IP₃ receptor (Sienaert et al., 1997), it is possible that the mutation reduces receptor activity by affecting calcium binding.

In an alternative model, the frequency of calcium oscillations may reflect the rate of IP₃ receptor recovery following inactivation of the receptor. Elevated calcium concentrations inhibit IP₃ receptor activity and prevent further calcium release from the channel, even in the presence of sustained levels of IP₃ (Bezprozvanny et al., 1991; Oancea and Meyer, 1996). While IP₃ receptors are inactive, calcium is pumped back into stores, returning cytosolic calcium to resting levels. The time spent in the inactive state could define the frequency of calcium spikes. Oancea and Meyer (1996) determined that in rat basophilic leukemia cells the half-maximal rate of recovery at peak calcium concentrations is about 30 s, and a subsequent spike is not triggered until a threshold number of IP₃ receptors return to a state that can be activated by calcium. In this model, *itr-1(sa73)* might decrease the frequency of calcium spikes by altering the recovery rate of the channel.

Although we describe the function of the IP₃ receptor as being an essential element of the timekeeper, neither of these models precludes a role for other proteins in the timekeeping mechanism. Specifically, these proteins might interact as a pathway or a cascade of protein interactions that form a cycle. There are at least 12 genes in addition to *itr-1* that alter the frequency of the defecation cycle when mutated (Iwasaki et al., 1995). Many of these are likely to encode modulatory elements; however, some may encode other essential components of the clock. For example, PLC is likely to play an essential role in IP₃ receptor activation rather than a modulatory role. In such a model, calcium from the IP₃ receptor might feed back on PLC activation and thus generate a self-sustaining oscillator between the activation of two proteins. To date, only one other gene affecting defecation cycle time has been cloned. The gene, *flr-1*, encodes a new member of the degenerin/epithelial sodium channel family of proteins (Take-uchi et al., 1998). Consistent with a role in regulating defecation cycle timing, the FLR-1 protein is expressed only in the intestine. These results suggest that *flr-1* regulates the membrane potential of intestinal cells and also implicate membrane excitability in the control of cycle timing.

Rhythmic Behaviors with Different Periodicities

The frequency of calcium oscillations triggered by IP₃ receptor activation often varies depending on the cell type. For example, calcium oscillations in some neuronal cells can occur with a relatively fast period ranging from milliseconds to a few seconds (MacVicar et al., 1987; Payne and Potter, 1991). Longer periods of a minute or more have been observed in oocytes following fertilization, in hepatocytes, and in macrophages (Cuthbertson and Cobbold, 1985; Kruskal and Maxfield, 1987; Woods et al., 1987). The expression pattern of the *itr-1* gene suggests that regulated calcium release via the IP₃ receptor might also be important for regulating behavioral rhythms with faster frequencies. Specifically, the *itr-1* gene is expressed in the isthmus of the pharynx and in the gonad sheath cells and spermatheca. Both of these tissues contract rhythmically. Isthmus peristalsis occurs

approximately every 1–2 s (Avery and Horvitz, 1987). Sheath cells contract about every 7 s (McCarter et al., 1997). Variations in the frequency of each behavior could arise from differences in stimulation of the receptor, for example, by variations in IP₃ production, or by differences in the expression of regulatory proteins acting on the IP₃ receptor.

Coordination of a Complex Multicellular Behavior

A surprising result from these studies is that the timekeeper for this motor program does not lie in neurons or muscles but rather is located in the intestine. How can IP₃ receptor–induced calcium oscillations in the intestine activate the muscles and neurons that mediate the defecation cycle? In neuroendocrine cells, calcium oscillations regulate periodic hormone secretions (Tse et al., 1993; Chow et al., 1994). It is likely that a similar mechanism triggers the secretion of a signal from the intestine. The anatomy of the intestine in *C. elegans* is well suited for the purpose of secreting intercellular signals (Wood, 1988). The intestine forms a tube of 20 cells coupled by gap junctions and runs along the length of most of the animal. In electron micrographs, we have observed an accumulation of vesicular structures near the plasma membrane of the posterior intestinal cells (E. M. J., unpublished data). We speculate that these may represent secretory vesicles containing a signal for initiating the posterior body contraction and activating the neurons that control the anterior body contraction and enteric muscle contraction. Alternatively, these structures may be calcium storage compartments close to the plasma membrane that play a role in the propagation of the calcium wave.

The anatomy of the intestine may be particularly important for the activation of the posterior body contraction. The body wall muscles are arranged in four longitudinal rows, two dorsal and two ventral, flanking the intestine. The posterior body contraction originates at the most posterior muscle and proceeds anteriorly as a wave of muscle contraction. One possible mechanism for the propagation of this muscle contraction is that a calcium wave is initiated in the most posterior intestinal cell and is propagated via gap junctions to adjacent intestinal cells. Each of these cells could then secrete a signal to the adjacent muscles so that the contraction of the body muscles parallels the calcium wave in the intestine. Another possibility is that calcium oscillations occur in a single posterior intestinal cell. This cell could then secrete a signal that either diffuses through the pseudocoelomic space or activates a posterior muscle, and a wave of contraction is propagated by the electrically coupled muscle cells.

A remarkable implication of these studies is that a single tissue, the intestine, independently activates each of the serial muscle contractions that comprise the behavior. In other organisms, calcium waves generally act to regulate activities of a single cell (e.g., during fertilization of an egg) or to initiate secretion from the cell that may have a slow effect on the organism (e.g., secretion from neuroendocrine cells). In *C. elegans*, the behavior of the animal is in lockstep with the activity of the IP₃ receptor. In other words, there is a one-to-one relationship between the calcium spike in the intestinal cells

and the execution of the posterior body muscle contraction. In addition, the intestine must activate a neural circuit that is required for the anterior body contraction and the enteric muscle contraction (McIntire et al., 1993). In the future, it will be important to determine the molecular mechanisms of signaling between calcium spikes in the intestine and the muscle and neuronal effectors of the behavior.

Experimental Procedures

Strains and Alleles

Standard methods for maintaining *C. elegans* strains were used as described by Brenner (1974). Bristol strain N2 was used as the wild type, and all animals were grown at room temperature unless otherwise stated. The following genetic markers and mutations were used in this study: LGI, *unc-29(e193)*; LGIII, *ncl-1(e1865)*; LGIV, *lin-45(n2018cs)*, *unc-24(e138)*, *itr-1(sa73)*; LGX, *lin-15(n765ts)*. *stDf7* is a deficiency on LGIV that removes markers flanking *itr-1*. All strains are available from the *C. elegans* Genetics Stock Center.

Genetic Analysis and Phenotypic Characterization

The *n2559* mutant allele was isolated by ethylmethane sulfonate mutagenesis in a screen for lethal mutations that was unrelated to this study. In the course of characterizing this mutant, we noticed that the larvae were extremely constipated and failed to initiate a defecation cycle. Standard three-factor mapping placed the *n2559* allele in the interval between *lin-45* and *unc-24* on LGIV. Two out of four Unc non-Lin animals segregated *n2559*. *n2559* animals were subsequently maintained as heterozygotes balanced by a *lin-45(n2018cs) unc-24(e138)* chromosome and grown at 15°C. *sa73* and *n2559* were tested for complementation by first crossing *n2559/lin-45(n2018) unc-24(e138)* heterozygotes to N2 males to generate *n2559/+* and *lin-45 unc-24/+* males. These heterozygous males were then crossed to *unc-29(e193); dec-4(sa73); ncl-1(e1865)* homozygous hermaphrodites. Non-Unc-29 cross progeny were cloned. Fourteen out of twenty non-Unc-29 clones segregated Dec+ and *unc-29; dec-4; ncl-1* progeny in subsequent generations but no *n2559* progeny. Six out of twenty non-Unc-29 clones had a long defecation cycle time, appeared severely constipated, and were sterile.

The defecation cycles of first day adult animals were scored for each genotype. Cycles were observed at 20°C, and time was measured from one posterior body contraction to the next. For each strain, a minimum of five different animals were scored for ten cycles each. *n2559* animals were scored for a period ranging between 20 min and 1 hr. Brood size was measured by cloning 15 L4 animals of each genotype. Animals were moved each day for 4 days to a new plate, and the resulting F1 progeny were counted.

Transformation Rescue and Cloning of *itr-1*

Transgenic strains were generated by standard techniques. Initial rescue was obtained by injecting either *itr-1(n2559)/lin-45(n2018cs) unc-24(e138)* heterozygotes or *sa73* animals with the cosmid R06H2 as well as with the plasmid pRF4, a marker for stable transformants (Mello et al., 1991). Five out of five *n2559* transgenic lines were fully rescued, and two out of two *sa73* lines were fully rescued. Three overlapping fragments amplified from N2 genomic DNA rescue the *n2559* mutant phenotype. The fragments include 7.5 kb of the 5' untranslated region, and the central fragment overlaps 789 bp and 475 bp at the 5' and 3' end, respectively. Partial rescue of *n2559* was also obtained with a gel-purified *NarI* restriction fragment that contains 5.8 kb of upstream sequence and 2.7 kb downstream of the *itr-1* gene. To identify the molecular lesions in *n2559* and *sa73*, genomic fragments about 3–5 kb in length were obtained by single worm PCR using a long-range PCR system (Boehringer Mannheim) for amplification. Regions corresponding to predicted exons were directly sequenced by an automated sequencing machine (Applied Biosystems) or manually sequenced with Thermo Sequenase cycle sequencing kit (Amersham).

The sequence of the *itr-1* transcript was obtained by reverse transcription of wild-type RNA followed by PCR amplification of

fragments about 2 kb in length. Fragments were then gel purified and sequenced directly by an automated sequencing machine. The 5' *trans*-spliced sequence was obtained by PCR amplification with an SL1 primer. The 3' sequence was obtained by PCR amplification with a pool of oligo dT primers in which the most 3' base was either A, C, or G.

Construction of the *itr-1::GFP* Reporter Gene

Standard molecular biological techniques were used to construct plasmids. A genomic subclone, pPD2, was generated by inserting a SacI/BamHI fragment from the cosmid R06H2 into Litmus 28 (New England Biolabs). The clone contains 8.2 kb of sequence upstream of the *itr-1* ATG start codon and 4.6 kb downstream of the ATG. GFP and the *unc-54* polyadenylation sequence from pPD95.85 (A. Fire, J. Ahnn, G. Seydoux, and S. Xu, personal communication) were amplified with primers tagged with a SapI site at the 5' end and a BssHII site at the 3' end. The PCR product was then cloned into the pCR2.1 TA cloning vector (Invitrogen) to generate the plasmid pPD4. The GFP fusion construct was made by ligating the SapI/BssHII fragment from pPD4 into pPD2. The resulting plasmid, pPD5, contains the *itr-1* promoter, the first 19 amino acids of ITR-1 followed by GFP and the *unc-54* terminator. *lin-15(n765ts)* animals were injected with pPD5 and pEK1 *lin-15(+)* DNA (Clark et al., 1994) to generate an extrachromosomal array (*oxEx104*) in the strain EG1526.

Mosaic Analysis of *itr-1*

We used the strain EG1394 *ncl-1(e1865); itr-1(n2559); oxEx75 [itr-1(+); ncl-1(+); sur-5::GFP]* to isolate *itr-1* genetic mosaics. EG1394 was generated by injecting *itr-1(n2559)/unc-24(e138) lin-45(n2018); ncl-1(e1865)* heterozygotes with R06H2, the cosmid C33C3 that rescues the *ncl-1* phenotype (Miller et al., 1996), and the *sur-5::GFP* plasmid pTG96 that causes expression of GFP in the nuclei of most somatic cells (Yochem et al., 1998). Animals of this strain were phenotypically wild type and segregated Ncl animals that had lost the array and were constipated due to defecation cycle defects (Dec). We picked constipated Dec animals from EG1394 and screened them using a dissecting microscope equipped with epifluorescence for GFP (Leica), looking for rare mosaics that had retained the *itr-1(+)* array in some cells, as indicated by GFP fluorescence. Mosaics due to early losses of the array were readily identified by patterns of *sur-5::GFP* fluorescence. The exact loss points in the mosaic animals were determined by scoring particular cells from multiple lineages for *sur-5::GFP* expression and Ncl using fluorescence and Nomarski optics (George et al., 1998).

We screened approximately 800 Dec animals from EG1394 and identified 23 mosaic animals in which the array had been lost in an interpretable pattern. Eight animals had lost the array in all cells derived from P₁ (class a). Strikingly, the remaining 11 Dec mosaic animals displayed patterns of mosaicism resulting from loss of the array in more than one cell during early embryogenesis (compound mosaicism). It was possible that *itr-1* function in the gut cells could be necessary but not sufficient to confer a strong Dec phenotype, that is, that loss in the gut and in some other cell was required to generate Dec animals. However, additional loss points were variable, and non-Dec animals also showed compound mosaicism, suggesting instead that the array was unstable. Finally, analysis of non-Dec animals demonstrated that expression in the gut was sufficient for function.

We also used the strain EG1520, of genotype *ncl-1; itr-1(n2559); oxEx98 [itr-1(+), ncl-1(+), rol-6(dm), sur-5::GFP]*, in additional screens for mosaic animals. The *oxEx98* array in EG1520 was generated in the same way as *oxEx75* except that it included the plasmid pRF4, which confers a Rol phenotype in transgenic animals. The Rol phenotype requires the dominant *rol-6* bearing array to be retained in AB-derived cells; thus, animals with losses in AB were non-Rol, and animals with losses in P₁ were Rol. We used this phenotype to screen for AB mosaics, which we found to be non-Rol, nonconstipated animals with disorganized gonads and protruding vulvas. Eight AB mosaics were identified, of which six were simple AB losses (class m) and two were compound mosaics (classes n and o). We scored defecation cycles in four of the six class m animals and both compound mosaic animals and found them to have normal timing, although three of the four AB mosaics displayed

a weak Aex or Exp phenotype. One mosaic with a P₁ loss and three mosaics with loss in E (in classes d, k, and l) were also identified in the EG1520 screen.

Calcium Imaging

Adult animals were injected in one of the two most posterior intestinal cells with a solution containing 2.4 mM fura-2 (fura dextran, potassium salt, 10,000 MW; Molecular Probes). After injection, animals were allowed to recover for a short time (1–4 hr) and were then prepared for imaging. Healthy animals were mounted on a 5% agarose pad containing 10 mM 5-HT to stimulate pharyngeal pumping. In the absence of 5-HT, the immobilized animals did not pump consistently. Animals that are not pumping suppress the defecation motor program (Liu and Thomas, 1994), and thus, in the absence of 5-HT we could not visually score cycle frequency. 5-HT accelerates the defecation cycle (E. M. J., unpublished data). Consistent with this effect of 5-HT, we observed a slight increase in the cycle frequency of some of the mounted animals in the presence of 5-HT compared to the freely behaving animals in the absence of 5-HT. The animals were immobilized by placing a spot of surgical glue (Histoacryl, B. Braun Surgical) on the dorsal surface such that only the posterior half of the animal was glued to the pad. A small amount of food was then placed near the mouth of the animal. The defecation cycle of animals that had been mounted on microscope slides were scored before imaging to confirm the health of the animals.

Ratio measurement of intracellular calcium was performed using MetaFluor software (Universal Imaging). Worms were imaged using a 40× Nikon objective on a Nikon Diaphot inverted microscope. Alternate excitation every 1.6–3 s at 340 nm and 380 nm wavelengths was performed using a Lambda-10 Filter Wheel Controller (Sutter Instruments). Excitation light was provided by a 75W Nikon Xenon lamp. Emitted light was collected through a dichroic mirror and 510 nm interference filters. Images were captured by a cooled CCD camera.

Acknowledgments

We thank NPS Pharmaceuticals and G. Shankar for the use of calcium imaging equipment; P. Guthrie and S. B. Kater for advice concerning calcium imaging; H. R. Horvitz, in whose laboratory the *n2559* allele was isolated; H. Baylis for communicating unpublished results; A. Fire for pPD95.85; M. Han for *sur-5::GFP*; M. Hammarlund for RNA; D. Hutcheson for cosmid; P. Sternberg for sending *lfe-1* and *lfe-2* alleles; J. Richmond and J. L. Bessereau for critical reading of the manuscript; and members of our laboratory for many insightful discussions. This work was supported by a grant from the National Institutes of Health to E. M. J. (NS 34307). P. D. S. was supported by the University of Utah Graduate Research Fellowship. A. D. C. is an Alfred P. Sloan Foundation Research Fellow in the Neurosciences. The *C. elegans* Genome Consortium provided cosmid, and some strains were provided by the Caenorhabditis Genetics Center.

Received May 17, 1999; revised July 16, 1999.

References

- Arshavsky, Y.I., Deliagina, T.G., and Orlovsky, G.N. (1997). Pattern generation. *Curr. Opin. Neurobiol.* 7, 781–789.
- Avery, L., and Horvitz, H.R. (1987). A cell that dies during wild-type *C. elegans* development can function as a neuron in a *ced-3* mutant. *Cell* 51, 1071–1078.
- Berridge, M.J. (1993). Inositol trisphosphate and calcium signaling. *Nature* 361, 315–325.
- Berridge, M.J. (1997). Elementary and global aspects of calcium signaling. *J. Physiol.* 499, 291–306.
- Bezprozvanny, I., Watras, J., and Ehrlich, B.E. (1991). Bell-shaped calcium-response curves of Ins(1,4,5)P₃- and calcium-gated channels from endoplasmic reticulum of cerebellum. *Nature* 351, 751–754.
- Brenner, S. (1974). The genetics of *Caenorhabditis elegans*. *Genetics* 77, 71–94.

- Calabrese, R.L. (1995). Oscillation in motor pattern-generating networks. *Curr. Opin. Neurobiol.* 5, 816–823.
- Chow, R.H., Klingauf, J., and Neher, E. (1994). Time course of Ca²⁺ concentration triggering exocytosis in neuroendocrine cells. *Proc. Natl. Acad. Sci. USA* 91, 12765–12769.
- Clandinin, T.R., DeModena, J.A., and Sternberg, P.W. (1998). Inositol trisphosphate mediates a RAS-independent response to LET-23 receptor tyrosine kinase activation in *C. elegans*. *Cell* 92, 523–533.
- Clark, S.G., Lu, X., and Horvitz, H.R. (1994). The *Caenorhabditis elegans* locus *lin-15*, a negative regulator of a tyrosine kinase signaling pathway, encodes two different proteins. *Genetics* 137, 987–997.
- Cuthbertson, K.S.R., and Cobbold, P.H. (1985). Phorbol ester and sperm activate mouse oocytes by inducing sustained oscillations in cell Ca²⁺. *Nature* 316, 541–542.
- Dunlap, J.C. (1993). Genetic analysis of circadian clocks. *Annu. Rev. Physiol.* 55, 683–728.
- Dunlap, J.C. (1999). Molecular bases for circadian clocks. *Cell* 96, 271–290.
- Edmunds, L.N. (1988). *Cellular and Molecular Bases of Biological Clocks* (New York: Springer-Verlag).
- Ferris, C.D., Cameron, A.M., Bredt, D.S., Haganir, R.L., and Snyder, S.H. (1991a). Inositol 1,4,5-trisphosphate receptor is phosphorylated by cyclic AMP-dependent protein kinase at serines 1755 and 1589. *Biochem. Biophys. Res. Commun.* 175, 192–198.
- Ferris, C.D., Haganir, R.L., Bredt, D.S., Cameron, A.M., and Snyder, S.H. (1991b). Inositol trisphosphate receptor: phosphorylation by protein kinase C and calcium calmodulin-dependent protein kinases in reconstituted lipid vesicles. *Proc. Natl. Acad. Sci. USA* 88, 2232–2235.
- Ferris, C.D., and Snyder, S.H. (1992). Inositol 1,4,5-trisphosphate-activated calcium channels. *Annu. Rev. Physiol.* 54, 469–488.
- Fleming, J.T., Baylis, H.A., Sattelle, D.B., and Lewis, J.A. (1996). Molecular cloning and *in vitro* expression of *C. elegans* and parasitic nematode ionotropic receptors. *Parasitology* 113, s175–s190.
- Furuichi, T., Yoshikawa, S., Miyawaki, A., Wada, K., Maeda, N., and Mikoshiba, K. (1989). Primary structure and functional expression of the inositol 1,4,5-trisphosphate-binding protein P400. *Nature* 342, 32–38.
- George, S.E., Simokat, K., Hardin, J., and Chisholm, A.D. (1998). The VAB-1 Eph receptor tyrosine kinase functions in neural and epithelial morphogenesis in *C. elegans*. *Cell* 92, 633–643.
- Giles, W., van Ginneken, A., and Shibata, E.F. (1986). Ionic currents underlying cardiac pacemaker activity: a summary of voltage-clamp data from single cells. In *Cardiac Muscle: The Regulation of Excitation Contraction Coupling*, R.D. Nathan, ed. (Orlando: Academic Press, Inc.), pp. 1–27.
- Hedgecock, E.M., and Herman, R.K. (1995). The *ncl-1* gene and genetic mosaics of *Caenorhabditis elegans*. *Genetics* 141, 989–1006.
- Iwasaki, K., and Thomas, J.H. (1997). Genetics in rhythm. *Trends Genet.* 13, 111–115.
- Iwasaki, K., Liu, D.W., and Thomas, J.H. (1995). Genes that control a temperature-compensated ultradian clock in *Caenorhabditis elegans*. *Proc. Natl. Acad. Sci. USA* 92, 10317–10321.
- Kruskal, B.A., and Maxfield, F.R. (1987). Cytosolic free calcium increases before and oscillates during frustrated phagocytosis in macrophages. *J. Cell Biol.* 105, 2685–2693.
- Liu, D.W., and Thomas, J.H. (1994). Regulation of a periodic motor program in *C. elegans*. *J. Neurosci.* 14, 1953–1962.
- MacVicar, B.A., Crichton, S.A., Burnard, D.M., and Tse, F.W.Y. (1987). Membrane conductance oscillations in astrocytes induced by phorbol ester. *Nature* 329, 242–243.
- Marder, E., and Calabrese, R.L. (1996). Principles of rhythmic motor pattern generation. *Physiol. Rev.* 76, 687–717.
- McCarter, J., Bartlett, B., Dang, T., and Schedl, T. (1997). Soma-germ cell interactions in *Caenorhabditis elegans*: multiple events of hermaphrodite germline development require the somatic sheath and spermathecal lineages. *Dev. Biol.* 181, 121–143.
- McIntire, S.L., Jorgensen, E.M., Kaplan, J., and Horvitz, H.R. (1993). The GABAergic nervous system of *Caenorhabditis elegans*. *Nature* 364, 337–341.
- Mello, C.C., Kramer, J.M., Stinchcomb, D., and Ambros, V. (1991). Efficient gene transfer in *C. elegans*: extrachromosomal maintenance and integration of transforming sequences. *EMBO J.* 10, 3959–3970.
- Mikoshiba, K., Furuichi, T., and Miyawaki, A. (1994). Structure and function of IP₃ receptors. *Semin. Cell Biol.* 5, 273–281.
- Miller, L.M., Waring, D.A., and Kim, S.K. (1996). Mosaic analysis using a *ncl-1*(+) extrachromosomal array reveals that *lin-31* acts in the Pn.p cells during *Caenorhabditis elegans* vulval development. *Genetics* 143, 1181–1191.
- Oancea, E., and Meyer, T. (1996). Reversible desensitization of inositol trisphosphate-induced calcium release provides a mechanism for repetitive calcium spikes. *J. Biol. Chem.* 271, 17253–17260.
- Payne, R., and Potter, B.V. (1991). Injection of inositol trisphosphorothioate into *Limulus* ventral photoreceptors causes oscillations of free cytosolic calcium. *J. Gen. Physiol.* 97, 1165–1186.
- Sienaert, I., Missiaen, L., De Smedt, H., Parys, J.B., Sipma, H., and Casteels, R. (1997). Molecular and functional evidence for multiple Ca²⁺-binding domains in the type 1 inositol 1,4,5-trisphosphate receptor. *J. Biol. Chem.* 272, 25899–25906.
- Takeuchi, M., Kawakami, M., Ishihara, T., Amano, T., Kondo, K., and Katsura, I. (1998). An ion channel of the degenerin/epithelial sodium channel superfamily controls the defecation rhythm in *Caenorhabditis elegans*. *Proc. Natl. Acad. Sci. USA* 95, 11775–11780.
- Thomas, J.H. (1990). Genetic analysis of defecation in *Caenorhabditis elegans*. *Genetics* 124, 855–872.
- Tse, A., Tse, F.W., Almers, W., and Hille, B. (1993). Rhythmic exocytosis stimulated by GnRH-induced calcium oscillations in rat gonadotropes. *Science* 260, 82–84.
- Wang, S.S., and Thompson, S.H. (1995). Local positive feedback by calcium in the propagation of intracellular calcium waves. *Biophys. J.* 69, 1683–1697.
- Wood, W.B. (1988). *The Nematode Caenorhabditis elegans* (Cold Spring Harbor, NY: Cold Spring Harbor Laboratory Press).
- Woods, N.M., Cuthbertson, K.S.R., and Cobbold, P.H. (1987). Phorbol-ester-induced alterations of free calcium ion transients in single rat hepatocytes. *Biochem. J.* 246, 619–623.
- Yochem, J., Gu, T., and Han, M. (1998). A new marker for mosaic analysis in *Caenorhabditis elegans* indicates a fusion between *hyp6* and *hyp7*, two major components of the hypodermis. *Genetics* 149, 1323–1334.
- Yoshikawa, S., Tanimura, T., Miyawaki, A., Nakamura, M., Yuzaki, M., Furuichi, T., and Mikoshiba, K. (1992). Molecular cloning and characterization of the inositol 1,4,5-trisphosphate receptor in *Drosophila melanogaster*. *J. Biol. Chem.* 267, 16613–16619.